Biosensors and Bioelectronics 26 (2011) 2442–2447

Contents lists available at ScienceDirect

Biosensors and Bioelectronics

journal homepage: www.elsevier.com/locate/bios

A folding-based electrochemical aptasensor for detection of vascular endothelial growth factor in human whole blood

Shuang Zhao[a,b], Weiwei Yang[b], Rebecca Y. Lai[b,*]

[a] College of Sciences, Northeastern University, Shenyang 110004, China
[b] Department of Chemistry, University of Nebraska-Lincoln, Lincoln, NE 68588-0304, USA

ARTICLE INFO

Article history:
Received 15 August 2010
Received in revised form 18 October 2010
Accepted 18 October 2010
Available online 23 October 2010

Keywords:
Vascular endothelial growth factor
Methylene blue
Aptamer
Alternating current voltammetry
Human whole blood

ABSTRACT

We herein report a folding-based electrochemical DNA aptasensor for the detection of vascular endothelial growth factor (VEGF) directly in complex biological samples, including blood serum and whole blood. The electrochemical signal generation is coupled to a large, target-induced conformational change in a methylene blue-modified and surface immobilized anti-VEGF aptamer. The sensor is sensitive, selective and essentially reagentless: we can readily detect VEGF down to 5 pM (190 pg/mL) directly in 50% blood serum. Similar to other aptasensors of this class, the VEGF sensor is also regenerable and reusable. In addition, the sensor performs comparably well even when fabricated on a gold-plated screen-printed carbon electrode and can potentially be implemented as a cost-effective, single-use biosensor for diseases diagnosis and therapy monitoring. The exceptional sensitivity, selectivity, and reusability of this electrochemical aptasensor platform suggest it may be a promising strategy for a wide variety of sensing applications.

1. Introduction

Vascular endothelial growth factor (VEGF) is a key regulator of both physiologic and pathologic angiogenesis. As its name suggests, VEGF stimulates vascular endothelial cell growth, survival, and proliferation (Ferrara, 2004; Hoeben et al., 2004). VEGF is a signaling protein that has been used as a serum biomarker for a number of human diseases, including cancer (Carmeliet and Jain, 2000; Plate et al., 1992; Salven et al., 1999), rheumatoid arthritis (Nakahara et al., 2003), psoriasis (Detmar, 2004) and proliferating retinopathy (Ray et al., 2004). For example, when tumors reach a size of about 0.2–2.0 mm in diameter, they need independent blood supplies for oxygen and nutrients to drive further growth and metastasis, which are acquired by the overexpression of VEGF, resulting in the creation and maintenance of a growing vascular network (Roskoski, 2007). Thus, rapid, selective and sensitive detection of VEGF directly in the patients' whole blood or serum is particularly important for disease diagnosis and subsequent therapy monitoring. To date, various VEGF detection techniques have been reported, including enzyme-linked immunosorbent assays (ELISAs), immunohistochemistry, radioimmunoassay and others; however, since these techniques are labor-intensive, time-consuming and require sophisticated instrumentations, they are therefore not ideal for near real-time clinical diagnostics.

Over the past three decades, antibodies have been the biorecognition element of choice in the development of biosensing assays, the emergence of a new class of biorecognition elements will undoubtedly change the long-standing dominance of antibodies-based detection approaches. In 1990, two labs independently developed the technique to select aptamers, also known as chemical antibodies, with of the goal of using them for both therapeutic and biosensing applications (Ellington and Szostak, 1990; Tuerk and Gold, 1990). Aptamers are single-stranded DNA, RNA or modified nucleic acids that have been designed through an *in vitro* selection process known as SELEX (systematic evolution of ligands by exponential enrichment), in which specific oligonucleotides are isolated from complex libraries of synthetic nucleic acids by repetitive binding of the oligonucleotides to target molecules (Ellington and Szostak, 1990; Tuerk and Gold, 1990). Aptamers possess high selectivity and affinity toward a wide range of targets, including metal ions (Jiang et al., 2009; Radi and O'Sullivan, 2006), small organic molecules (Swensen et al., 2009), proteins (Tang et al., 2007) and even whole cells (Shangguan et al., 2006). Aptamers offer several advantages over antibodies, including the ease of synthesis, easy labeling and good stability. Given these attributes, aptamers have recently been regarded as highly promising biorecognition elements in sensor design. Thus motivated, various aptamer-based sensors (aptasensor) have been realized,

* Corresponding author at: Department of Chemistry, University of Nebraska-Lincoln, 651 Hamilton Hall, Lincoln, NE 68588-0304, USA. Tel.: +1 402 472 5340; fax: +1 402 472 9402.
E-mail address: rlai2@unl.edu (R.Y. Lai).

0956-5663/$ – see front matter © 2010 Elsevier B.V. All rights reserved.
doi:10.1016/j.bios.2010.10.029

encompassed almost every possible biosensing strategies, including optical, electrochemical, and mass-sensitive approaches (Cho et al., 2009; Hianik and Wang, 2009; Song et al., 2008; Willner and Zayats, 2007).

Electrochemical aptasensors have gained substantial popularity since 2004 (Ikebukuro et al., 2004), and among these sensors, the folding-based aptasensors have warranted more attention, owing to the merits associated with this sensing platform (Acero Sánchez et al., 2006; Baker et al., 2006; Lai et al., 2007; Radi et al., 2006; Xiao et al., 2005a,b). Most sensors of this class are essentially reagentless, rapid, reusable, sensitive, specific, selective and are highly compatible with microfluidic-based detection platforms (Swensen et al., 2009). While various folding-based aptasensors have been developed for the detection of proteins and small molecules (Acero Sánchez et al., 2006; Baker et al., 2006; Lai et al., 2007; Radi et al., 2006; Xiao et al., 2005a,b), none have been developed for direct sensing of VEGF, an important serum biomarker relevant to various disease states. In this study, we developed a folding-based electrochemical aptasensor for detection of VEGF in complex, clinically relevant media. The aptamer employed here is the first anti-VEGF DNA aptamer reported in the literature (Potty et al., 2009; Taylor et al., 2008). Unlike Pegaptanib (Macugen) (Gold and Janjic, 1998) – the most widely-used and well-characterized anti-VEGF RNA aptamer – the DNA aptamer used in this study has the advantage of being more resistant to nuclease degradation. In addition, the aptamer discussed here provides a simple 1 (aptamer):1(VEGF) binding motive, contrary to other VEGF inhibitors that exhibit 2(ligands):1(VEGF) stoichiometry (Potty et al., 2009; Taylor et al., 2008). Most importantly, the unique folding motive of this DNA aptamer allows us to design a sensor that can translate target-induced conformational change directly into a measurable electrochemical signal change. This target-induced folding motive is well-suited for the construction of a "signal-on" sensor (Baker et al., 2006; Lai et al., 2007), thus circumventing the general disadvantages of "signal-off" sensors, in which only 100% signal suppression can be realized even under optimized conditions. A simple "signal-on" sensor architecture without the need of competitive binding and target-induced displacements will, undoubtedly, enhance the applicability of this sensor in near real-time VEGF detection for diseases diagnosis and therapy monitoring.

2. Materials and methods

2.1. Reagents

The thiol- and methylene blue (MB)-modified 28-mer anti-VEGF DNA aptamer (5′-HS-$(CH_2)_6$-TTCCCGTCTTCCAG-ACAAGAGTGCAGGG-$(CH_2)_7$-MB-3′) was used as the probe in this study. It was designed with the help of the mFold software as previous reported (Potty et al., 2009; Taylor et al., 2008) and was purchased from Biosearch Technologies, Inc. (Novato, CA). Recombinant human $VEGF_{165}$ (MW 38.2 kDa, pI = 8.5) purchased from Shenandoah Biotechnology, Inc. (Warwick, PA) was reconstituted in ultrapure water prior to use. Sulfuric acid, tris(2-carboxyethyl)phosphine hydrochloride (TCEP), 6-mercapto-1-hexanol (C6-OH), iron-supplemented fetal calf-serum, sodium dodecyl sulfate (SDS), and guanidine hydrochloride (GHCl) were purchased from Sigma–Aldrich (St. Louis, MO) and used without further purification. Human male whole blood obtained from Innovative Research (Novi, MI) was used as received. All other reagents were of analytical grade and used as received. The buffer solution used in this study was a 10 mM, pH 7.4 phosphate buffer supplemented with 0.1 M NaCl (PBS). Ultrapure water from a Synergy® water purification system (18.2 MΩ cm, Millipore, Billerica, MA) was used in all experiments.

2.2. Electrochemical measurements

All electrochemical measurements were performed in a conventional three-electrode system using a CHI 1040A Electrochemical Workstation (CH Instruments, Austin, TX). Polycrystalline gold disk electrodes (CH Instruments, Austin, TX) with geometric area of 0.0314 cm^2 were used as working electrodes. A platinum wire electrode and a Ag/AgCl (3 M KCl) electrode (both from CH Instruments, Austin, TX) were used as the counter electrode and reference electrode, respectively. For the strip-based electrochemical aptasensors, screen-printed carbon electrodes (SPCE) (Pine Instrument, Grove City, PA) consisted of a 2 mm diameter screen-printed carbon working electrode, a screen-printed Ag/AgCl reference electrode and a screen-printed carbon counter electrode were used as sensor substrates. The sensors were analyzed using alternating current voltammetry (ACV) over the potential range of −0.05 and −0.5 V (vs. Ag/AgCl) with a frequency of 10 Hz, amplitude of 25 mV AC potential. The density of aptamer probes on the electrode surface was determined using ACV as described in reference (Sumner et al., 2000). For calculation of the electron transfer rate constant (k_s) of MB, a series of cyclic voltammetric (CV) scans were conducted before and after target interrogation. To determine k_s after target interrogation, a saturating target concentration (50 nM) was used and the signal was allowed to reach complete saturation (1.5 h) prior to the collection of the CV scans. The CV peak potential separations ($\Delta E_p = E_{p,a} - E_{p,c}$) increase with the increase of scan rates (ν). When $\Delta E_p > 200/n$ mV, a graph of ΔE_p as a function of log ν yields a straight line which is in accordance with the Laviron equation (Laviron, 1979):

$$\log k_s = \alpha \log(1-\alpha) + (1-\alpha)\log\alpha - \log\left(\frac{RT}{nF\nu}\right) - \frac{\alpha(1-\alpha)nF\Delta E_p}{2.3RT} \quad (1)$$

where k_s is the apparent electron transfer rate constant (s^{-1}), α is the electron transfer coefficient, ν is the CV potential scan rate (V/s), and ΔE_p is the CV potential separations (V). The α value can be determined from the slope of the straight line, and k_s can be calculated with the help of the intercept. The ratio between the increase of peak current upon target binding and the peak current in the absence of target was used to calculate the % signal gain (Eq. (2)):

$$\text{signal gain}\,(\%) = \frac{I - I_0}{I_0} \quad (2)$$

where I is the baseline-subtracted peak current obtained in presence of the target, and I_0 is the baseline-subtracted peak current in the target-free solution. Unless specifically mentioned, all experiments were conducted at room temperature (~23 °C).

2.3. Preparation of an electrochemical aptasensor

Prior to sensor fabrication, the gold disk electrodes were polished successively with a 1.0 and 0.1 μm diamond slurry on a clean polishing microcloth (Buehler, Lake Bluff, IL). After each polishing step, the electrodes were rinsed with ultrapure water and sonicated in a low power sonicator for approximately 5 min to remove bound particulates. They were then electrochemically cleaned by a series of oxidation and reduction cycles in 0.5 M H_2SO_4 and 0.05 M H_2SO_4, respectively, until a cyclic voltammogram characteristic of the clean gold electrode could be obtained. To fabricate the sensor, 2 μL aptamer stock solution (0.2 mM) was incubated with 2 μL tris(2-carboxyethyl)phosphine hydrochloride (10 mM) for 1 h to cleave the disulfide bonds of the probe aptamer. This solution was then diluted to the appropriate aptamer concentration with PBS. Probe immobilization was achieved by immersing the cleaned electrodes into aptamers solution of various concentrations for 1 h.

The electrodes were then rinsed with ultrapure water and subsequently passivated with 2 mM 6-mercapto-1-hexanol overnight to displace any nonspecifically bound material. For the fabrication of a strip-based sensor, a gold film was first electrodeposited on the carbon working electrode by holding it at −0.4 V (vs. Ag/AgCl) in a stirred gold solution (1.2 mg/mL $HAuCl_4$, 1.5 wt.% HCl and 0.1 M NaCl) for 20 min (Yang et al., 2009). The resulting SPCE undergoes the same electrochemically cleaning and sensor fabrication process as mentioned previously.

3. Results and discussion

Aptamers are capable of folding into unique three-dimensional conformations upon binding to their targets. Recently, several successful electrochemical aptasensors have been designed based on this strategy (Acero Sánchez et al., 2006; Baker et al., 2006; Lai et al., 2007; Radi et al., 2006; Xiao et al., 2005a,b; Ferapontova et al., 2008; Zuo et al., 2007). In this study, the aptasensor is fabricated by covalently attaching a MB modified aptamer to a gold electrode via self-assembly alkanethiol chemistry. In the absence of target, the aptamer is thought to be partially unfolded; thereby obstructing electron transfer between the terminal MB label and the electrode surface, suppressing the faradaic current (Scheme 1, left). Upon VEGF binding, the aptamer is thought to fold into the conformationally restricted stem-loop structure, and this conformational change forces the MB label to be in close proximity with the electrode, resulting in a significant increase in electron transfer efficiency (Scheme 1, right).

3.1. Sensor response and binding kinetics

To understand the target-induced folding motive presumably present in this sensor architecture, we first interrogated the sensor in a pH 7.4 PBS using ACV. In the absence of VEGF, a well-defined electrochemical reduction peak originating from the MB redox label is observed at −0.28 V (vs. Ag/AgCl). The relatively low electrochemical signal could be due to the partially open conformation of the aptamer probe, which is known to obstruct efficient electron transfer (Lai et al., 2007). However, in the presence of 100 nM VEGF, the peak current increases by 135.0 ± 5.9%, owing to the formation of a rigid stem-loop structure in the aptamer, allowing the MB label to be closer to the electrode and thus enhances the MB redox signal (Supplementary Fig. S1A). In addition, target binding occurs rather rapidly, the majority of the response is achieved within 20 min although complete signal saturation time is ~60 min (Fig. 2). Of note, since the interfacial electron transfer rate is highly

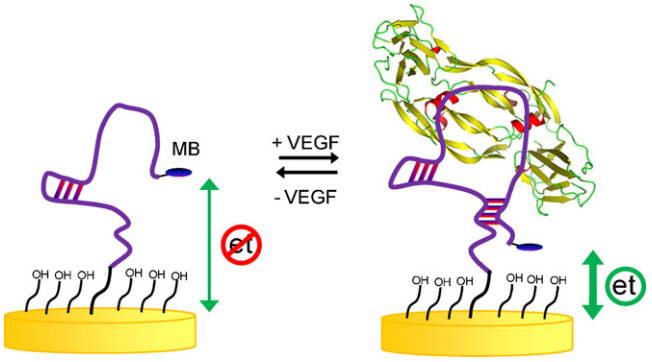

Scheme 1. The proposed sensing mechanism of the VEGF aptasensor. In the absence of target (left), the aptamer remains partially unfolded. Upon target binding (right), the aptamer is thought to fold into a conformation which holds the MB label in close proximity to the electrode, thus increasing the observed faradaic current.

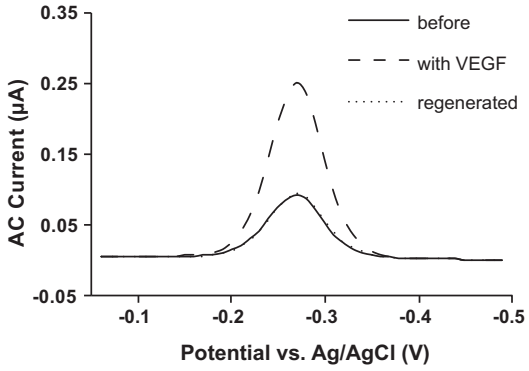

Fig. 1. Sensor response in undiluted human whole blood. Shown are baseline-subtracted AC voltammograms for the sensor before (solid curve), after incubation with 100 nM VEGF (dashed curve), and after regeneration with 8 M GHCl (dotted curve).

dependent on the distance between the MB redox moiety and the electrode surface, using the Laviron equation (Laviron, 1979) we calculated the k_s value of MB before and after interacting with VEGF. The k_s value obtained in absence and presence of VEGF are 34 s^{-1} and 140 s^{-1}, respectively. For this class of sensors, in addition to the change in probe dynamics which leads to an increase in the MB peak current, the observed increase in k_s upon target binding clearly suggests a change in the aptamer conformation, resulting in a decrease in distance between the redox label and the electrode. This change in the k_s value could potentially be used in determining the signaling mechanism in folding-based electrochemical biosensors.

Both the increase in AC current and k_s value upon VEGF binding suggest the presence of a target-induced conformational change in the aptamer, rather than non-specific adsorption of the protein to the sensor surface. The sensor should, therefore, be selective enough to be employed directly in realistically complex and contaminant-ridden media. To verify this claim, we interrogated the sensor in serum, the most commonly used clinical sample. As shown in Supplementary Fig. S1B, the characteristic reduction peak of MB shifts to −0.31 V (vs. Ag/AgCl) when interrogated in 50% fetal calf serum (diluted 1:1 with PBS), attributed to the slightly alkaline pH of serum and the strong pH dependence of MB reduction. In the presence of 100 nM VEGF, the signal increases by 130.2 ± 10.5%. While serum is used in most sensor applications, some point-of-case diagnostics may benefit greatly from utilizing minimally processed whole blood samples. Furthermore, the concentrations and properties of cellular and extra-cellular constituents in whole blood remain relatively unaltered when compare with their *in vivo* state. To our knowledge, few electrochemical aptasensors have been employed directly in undiluted whole blood. Thus, to further validate the sensor's selectivity, we challenged the sensor in undiluted human whole blood and find that it performs comparably well (Fig. 1). The signal gain is 177.8 ± 2.3%, slightly higher than that obtained in 50% serum. The difference is presumably due to the presence of a small amount of human VEGF in the whole blood used in the assay and the reasons behind this observation is currently under investigation in our lab (Mahner et al., 2010; Mitsuhashi et al., 2005; Di Raimondo et al., 2001). Of note, when compared to other commonly employed VEGF detection strategies, such as ELISAs (operation time of ~3 h), the response of this sensor is fairly rapid. For example, when interrogated in 50% serum, the sensor reaches signal saturation in ~50 min, with majority of signal change occurs within minutes (Fig. 2). Even in human whole blood, which has greater viscosity and could attenuate the diffusion of target to the surface of electrode, the binding kinetics is likewise expeditious (Fig. 2).

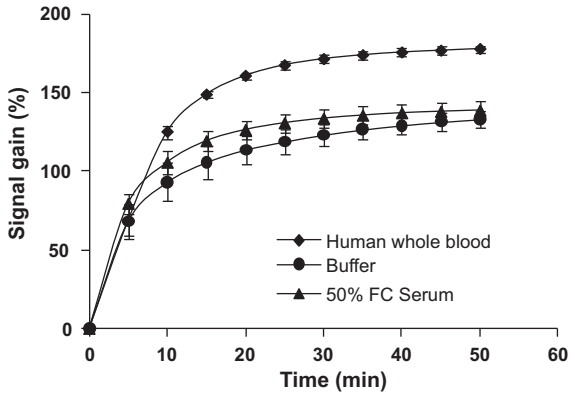

Fig. 2. Relatively rapid aptasensor. Shown is the typical sensor response after the introduction of 100 nM VEGF in buffer (●), 50% FC Serum (▲), and undiluted human whole blood (♦). The error bars represent one standard deviation from the mean, as calculated from three different sensors with similar probe density.

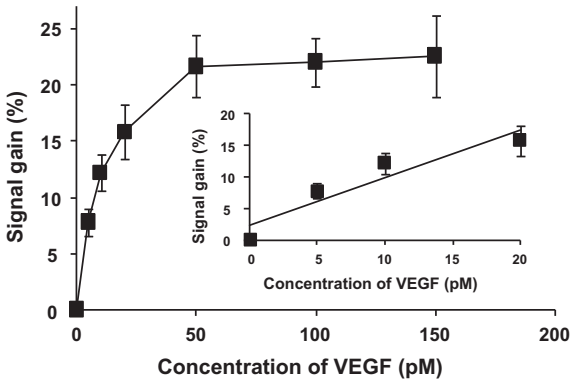

Fig. 3. Dose–response curves of the VEGF sensor in 50% serum. The concentration of thiolated oligonucleotide employed during sensor fabrication was 0.01 μM. The error bars represent one standard deviation from the mean, as calculated from three different sensors with similar probe density. The incubation time was 1 h and the interrogation temperature was 5 °C.

3.2. Sensor sensitivity and dynamic range

Similar to previously reported results, we find that surface probe density has a strong effect on sensor sensitivity and dynamic range (White et al., 2008). While probe density can be controlled by varying the concentration of the thiolated aptamer used in sensor fabrication, for this sensor, maximum achievable probe density of $\sim 7.3 \times 10^{11}$ molecules/cm^2 is obtained at probe concentration of ~0.5 μM. Higher probe density cannot be realized owing to the steric resistance and electrostatic repulsion between the negatively charged aptamers (White et al., 2008). Sensors with lower probe density exhibits lower MB reduction current in ACV, however, we find that the relative signal change upon target binding is significantly amplified (Xiao et al., 2005b), suggesting an enhancement in sensor sensitivity. Owing to the incompact arrangement which endows each probe with enough room to obtain favorable orientations to interact with targets and eliminates unfavorable interactions between the aptamer probes due to proximity, we could presumably achieve a lower limit of detection with sensors with lower probe density. However, with lower surface probe density, fewer aptamers are available for target binding, thus limiting the dynamic range of the sensor itself. This drawback, unfortunately, is commonly observed among protein sensors of this class, the goal here is to optimize the probe coverage according to the expected detection limit, which is highly contingent on the physiological concentration of the target species. For this sensor, to achieve an optimized probe density of $\sim 6.4 \times 10^{10}$ molecules/cm^2, 0.01 μM aptamer was employed in the fabrication step. As shown in Supplementary Fig. S2A, the sensor shows optimal sensor performance even when interrogated in 50% blood serum, achieving a detection limit as low as 50 pM. The linear dynamic range, however, is relatively limited, ranging from 50 pM to 0.15 nM. Sensors fabricated with a higher probe concentration (~0.1 μM) shows a larger linear dynamic range, covering concentrations between 200 pM and 5 nM, however, at the expense of the detection limit (200 pM) (Supplementary Fig. S2B). While a large dynamic range has various advantages, a low detection limit is sought after in this sensing application since the physiological concentration of VEGF in blood is relatively low (Mahner et al., 2010; Mitsuhashi et al., 2005; Raimondo et al., 1999).

Based on our studies with the electrochemical DNA sensor which shows a temperature-dependency in the sensor's signaling efficiency (data not shown), we presume that the sensitivity of the VEGF sensor can also be affected by sensor interrogation temperature. To verify our assumption, we tested the sensor's signaling efficiency at various temperatures (i.e., between −5 and 40 °C) (Supplementary Fig. S3). We notice an increase in MB reduction current with increasing temperatures, the change in the current, however, is completely reversible in which the same AC voltammogram could be obtained once the temperature source is removed. Similarly, a decrease in the MB current is evident when the temperature is lowered from room temperature (~23 °C), owing to the temperature-induced probe rigidity which dampens collisional electron transfer between the MB label and the electrode. It is therefore possible that the sensitivity of the VEGF sensor could be improved if interrogated at a low temperature, benefited from enhanced probe rigidity in the unbound state, leading to a larger overall signal difference between the unbound and bound state. This assumption has been verified – when challenged in 50% serum at 5 °C, the sensor achieves a detection limit of 5 pM (190 pg/mL), a detection limit that is within the physiological concentration of VEGF in human blood which averages from 256 pg/mL among healthy individuals to 434 pg/mL among cancer patients. (Fig. 3) (Mahner et al., 2010; Mitsuhashi et al., 2005; Raimondo et al., 1999). However, it is apparent that the linear dynamic range is more limited, presumably due to the combined effect of slower binding kinetics at lower temperature and general sensor behavior irreproducibility, which is often observed with this class of sensor when extremely low target concentrations are utilized. Despite minor differences in sensor behavior reproducibility, here we have clearly demonstrated the feasibility of adjusting the sensor's sensitivity and dynamic range by simply optimizing the probe density and interrogation temperature.

3.3. Sensor regenerability and reusability

Similar to other aptasensors of this class, this sensor is readily regenerable and reusable. To optimally regenerate the sensor, several known regeneration reagents (i.e., 25 mM NaOH, 10% SDS, 2 M KCl, 8 M GHCl, and 2 M NaSCN) were used in this study. After incubating in the regeneration reagent, the now VEGF-free sensor was placed in buffer, 50% serum or human whole blood in which a post-regeneration AC voltammogram was collected. Our results indicate that all the regeneration reagents employed in this study are highly effective, with current recovery of ~100% commonly observed. Even sensors interrogated directly in serum or human whole blood show similar sensor regenerability and stability. For example, we achieved 101.9 ± 4.6% (n = 6) signal recovery for sensors interrogated in 50% serum and regenerated with GHCl. However, since we are also interested in the sensor's reusability (i.e., post-regeneration VEGF binding efficiency), 8 M GHCl has proven to be the most effective among the five regeneration reagents and was thus used

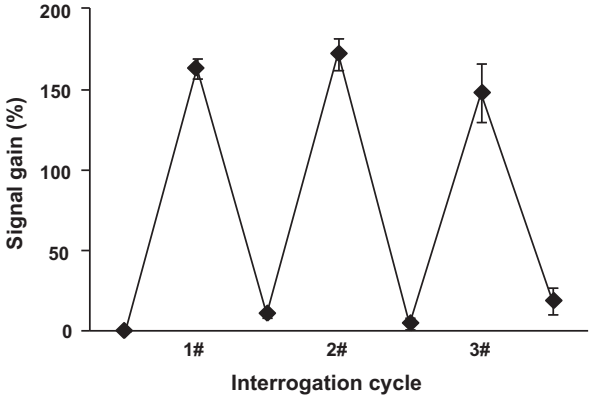

Fig. 4. Typical interrogation-regeneration plot of a VEGF sensor when challenged in undiluted human whole blood. The concentration of VEGF used in this experiment was 100 nM, with an incubation time of 1 h. The sensors were regenerated via a simple 5-min incubation in 8 M GHCl. The error bars represent one standard deviation from the mean, as calculated from three different sensors with similar probe density.

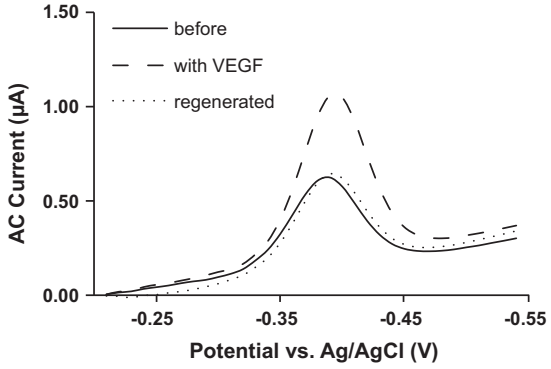

Fig. 5. Baseline-subtracted AC voltammograms of a sensor fabricated on a gold-plated screen-printed carbon electrode before (solid curve), after incubation with 100 nM VEGF (dashed curve), and after regeneration (dotted curve). In this experiment, the concentration of thiolated oligonucleotide employed during sensor fabrication was 0.5 μM.

in the remaining study (Fig. 1). However, even with GHCl as the regeneration reagent, signal reproducibility over 3 interrogations cannot be readily obtained (Fig. 4, Supplementary Fig. S4). One possible reason behind the observed reduction of signal gain with every use is aptamer degradation, especially when employed in serum or whole blood. This aptamer, like any DNA sequences, is prone to rapid degradation by nucleases present in the serum or whole blood, the problem, however, could be circumvented by employing Spiegelmers, L-oligonucleotide aptamers that are not subjected to enzymatic degradation (Eulberg and Klussmann, 2003; Klussmann et al., 1996). Of note, while some studies have suggested the lack of sensor-to-sensor reproducibly in this class of sensors (Lai et al., 2007), our results suggest otherwise, as illustrated by the small standard deviations shown in Fig. 4 and Supplementary Fig. S4.

3.4. VEGF sensor on gold-plated screen-printed carbon electrode

While some established sensor platforms for detection of VEGF exhibit superb sensitivity (Li et al., 2007; Prabhulkar et al., 2009), the realization of a cost-effective and mass producible sensor device, one that could operate directly in complex, multicontaminant samples is still a considerable challenge. Here we show that the VEGF sensor can be readily fabricated on a gold-plated screen-printed carbon electrode strip. For the strip-based sensor, we employed a custom-built electrochemical cell with a cell volume of 200 μL, thus improving sample efficiency and portability of the sensor. As shown in Fig. 5, when employed in 50% serum, due to the difference in the reference electrode potential, a more negative MB reduction potential (−0.39 V vs. screen-printed Ag/AgCl reference electrode) is observed. In the presence of 100 nM VEGF, the signal increases by 86%, lower than that observed in sensors fabricated on gold disk electrodes. The difference in signal gain could be due to the differences in probe coverage and probe orientations, which are often associated with the high surface roughness observed in gold-plated electrodes (Yang et al., 2009). Of note, the strip-based sensor is comparably reusable and can be regenerated via a 5-min incubation in 8 M GHCl. While the signaling efficiency can be further optimized, these results suggest that the strip-based aptasensor can potentially be implemented as a single-use biosensor for the detection of VEGF in point-of-care diagnosis.

4. Conclusions

We report, for the first time, a folding-based electrochemical aptasensor for rapid and sensitive detection of VEGF, a prominent biomarker associated with various disease states. Since the electrochemical signaling mechanism is linked to a target-induced conformational change of the aptamer probe, the sensor is thus highly resistive to nonspecific binding of matrix contaminants. It has demonstrated unprecedented selectivity, achieving direct VEGF detection at physiologically relevant levels in realistically complex media. Moreover, owing to the fully covalent sensor architecture, it is readily regenerable and reusable. Last, we have also demonstrated that this approach, as evident by the sensor's performance on a gold-plated carbon electrode strip, is well-suited to be implemented as a cost-effective, single-use biosensor for diseases diagnosis and therapy monitoring.

Acknowledgements

This study was supported by the University of Nebraska-Lincoln and Nebraska ESPCoR (EPS-0701892).

Appendix A. Supplementary data

Supplementary data associated with this article can be found, in the online version, at doi:10.1016/j.bios.2010.10.029.

References

Acero Sánchez, J.L., Baldrich, E., Radi, A.E., Dondapati, S., Sánchez, P.L., Katakis, I., O'Sullivan, C.K., 2006. Electroanalysis 18, 1957–1962.
Baker, B.R., Lai, R.Y., Wood, M.S., Doctor, E.H., Heeger, A.J., Plaxco, K.W., 2006. J. Am. Chem. Soc. 128, 3138–3139.
Carmeliet, P., Jain, R.K., 2000. Nature 407, 249–257.
Cho, E.J., Lee, J.-W., Ellington, A.D., 2009. Annu. Rev. Anal. Chem. 2, 241–246.
Di Raimondo, F., Azzaro, M.P., Palumbo, G.A., Bagnato, S., Stagno, F., Giustolisi, G.M., Cacciola, E., Sortino, G., Guglielmo, P., Giustolisi, R., 2001. Leukemia 15, 976–980.
Detmar, M., 2004. J. Invest. Dermatol. 122, xiv–xv.
Ellington, A.D., Szostak, J.W., 1990. Nature 346, 818–822.
Eulberg, D., Klussmann, S., 2003. Chem. Biol. Chem. 4, 979–983.
Ferapontova, E.E., Olsen, E.M., Gothelf, K.V., 2008. J. Am. Chem. Soc. 130, 4256–4258.
Ferrara, N., 2004. Endocr. Rev. 25, 581–611.
Gold, L., Janjic, N., NeXstar Pharmaceuticals, Inc. Boulder, Co, USA. US Patent 669625 (1998).
Hianik, T., Wang, J., 2009. Electroanalysis 21, 1223–1235.
Hoeben, A., Landuyt, B., Highley, M.S., Wildiers, H., Van Oosterom, A.T., De Bruijin, E.A., 2004. Pharmacol. Rev. 56, 549–580.
Ikebukuro, K., Kiyohara, C., Sode, K., 2004. Anal. Lett. 37, 2901–2909.
Jiang, Z., Fan, Y., Chen, M., Liang, A., Liao, X., Wen, G., Shen, X., He, X., Pan, H., Jiang, H., 2009. Anal. Chem. 81, 5439–5445.

Klussmann, S., Nolte, A., Bald, R., Erdmann, V.A., Furste, J.P., 1996. Nat. Biotechnol. 14, 1112–1115.
Lai, R.Y., Plaxco, K.W., Heeger, A.J., 2007. Anal. Chem. 79, 229–233.
Laviron, E., 1979. J. Electroanal. Chem. 101, 19–28.
Li, Y., Lee, H.J., Corn, R.M., 2007. Anal. Chem. 79, 1082–1088.
Mahner, S., Woelber, L., Eulenburg, C., Schwarz, J., Carney, W., Jaenicke, F., Milde-Langosch, K., Mueller, V., 2010. BMC Cancer 10, 139–151.
Mitsuhashi, A., Suzuka, K., Yamazawa, K., Matsui, H., Seki, K., Sekiya, S., 2005. Cancer 103, 724–730.
Nakahara, H., Song, J., Sugimoto, M., Hagihara, K., Kishimoto, T., Yoshizaki, K., Nishimoto, N., 2003. Arthritis Rheum. 48, 1521–1529.
Plate, K.H., Breier, G., Weich, H.A., Risau, W., 1992. Nature 359, 845–848.
Potty, A.S.R., Kourentzi, K., Fang, H., Jackson, G.W., Zhang, X., Legge, G.B., Willson, R.C., 2009. Biopolymers 91, 145–156.
Prabhulkar, S., Alwarappan, S., Liu, G., Li, C.-Z., 2009. Biosens. Bioelectron. 24, 3524–3530.
Radi, A.E., Acero Sánchez, J.L., Baldrich, E., O'Sullivan, C.K., 2006. J. Am. Chem. Soc. 128, 117–124.
Radi, A.E., O'Sullivan, C.K., 2006. Chem. Commun. 32, 3432–3434.
Ray, D., Mishra, M., Ralph, S., Read, I., Davies, R., Brenchley, P., 2004. Diabetes 53, 861–864.
Roskoski Jr., R., 2007. Crit. Rev. Oncol. Hematol. 62, 179–213.
Salven, P., Orpana, A., Joensuu, H., 1999. Clin. Cancer Res. 5, 487–491.
Shangguan, D., Li, Y., Tang, Z., Cao, Z.C., Chen, H.W., Mallikaratchy, P., Sefah, K., Yang, C.J., Tan, W., 2006. Proc. Natl. Acad. Sci. U.S.A. 103, 11838–11843.
Song, S., Wang, L., Li, J., Fan, C., Zhao, J., 2008. TRAC 27, 108–117.
Sumner, J.J., Weber, K.S., Hockett, L.A., Creager, S.E., 2000. J. Phys. Chem. B 104, 7449–7454.
Swensen, J.S., Xiao, Y., Ferguson, B.S., Lubin, A.A., Lai, R.Y., Heeger, A.J., Plaxco, K.W., Soh, H.T., 2009. J. Am. Chem. Soc. 131, 4262–4266.
Tang, J., Yu, T., Guo, L., Xie, J., Shao, N., He, Z., 2007. Biosens. Bioelectron. 22, 2456–2463.
Taylor, J.N., Darugar, Q., Kourentzi, K., Willson, R.C., Landes, C.F., 2008. Biochem. Biophys. Res. Commun. 373, 213–218.
Tuerk, C., Gold, L., 1990. Science 249, 505–510.
White, R.J., Phares, N., Lubin, A.A., Xiao, Y., Plaxco, K.W., 2008. Langmuir 24, 10513–10518.
Willner, I., Zayats, M., 2007. Angew. Chem. Int. Ed. 46, 6408–6418.
Xiao, Y., Lubin, A.A., Heeger, A.J., Plaxco, K.W., 2005a. Angew. Chem. 117, 5592–5595.
Xiao, Y., Piorek, B.D., Plaxco, K.W., Heeger, A.J., 2005b. J. Am. Chem. Soc. 127, 17990–17991.
Yang, W., Gerasimov, J.Y., Lai, R.Y., 2009. Chem. Commun. 20, 2902–2904.
Zuo, X., Song, S., Zhang, J., Pan, D., Wang, L., Fan, C., 2007. J. Am. Chem. Soc. 129, 1042–1043.